Desalination 262 (2010) 43–49

Contents lists available at ScienceDirect

Desalination

journal homepage: www.elsevier.com/locate/desal

Equilibrium and thermodynamic studies of Cu(II) removal by iron oxide modified sepiolite

E. Eren *, H. Gumus, N. Ozbay

Bilecik University, Faculty of Arts and Science, Department of Chemistry, 11210 Bilecik, Turkey

ARTICLE INFO

Article history:
Received 11 December 2009
Received in revised form 24 May 2010
Accepted 25 May 2010
Available online 1 July 2010

Keywords:
Sepiolite
Adsorption
Thermodynamic
Clay
Copper ions

ABSTRACT

This paper presents the adsorption of Cu(II) from aqueous solution by raw sepiolite (RS) and iron oxide-coated sepiolite (ICS) samples. Adsorption of Cu(II) by sepiolite samples was investigated as a function of the initial Cu(II) concentration, solution pH, ionic strength, temperature and the presence of an inorganic ligand (Cl^-, SO_4^{2-} and HPO_4^{2-}). Changes in the surface and structure were characterized by means of XRD, IR and XRF techniques. The Langmuir monolayer adsorption capacities of RS and ICS in 0.1 M $NaNO_3$ solution at 298 K were estimated to be 14.96 and 21.56 mg/g, respectively. ΔG, ΔH and ΔS were evaluated for RS and ICS to be −14.14 kJ/mol (at 298 K), 39.03 kJ/mol and 178 J/mol K, and −16.09 kJ/mol (at 298 K), 32.99 kJ/mol and 165 J/mol K, respectively.

1. Introduction

The contamination of water by heavy metals through the discharge of industrial wastewater is a worldwide environmental problem. The main heavy metal removal methods are chemical precipitation, membrane filtration, ion exchange and adsorption [1]. Adsorption processes provide attractive alternative treatment options to other removal techniques because they are more economical and readily available. A lot of non-conventional, low-cost and easily obtainable adsorbents have been tested for heavy metal removal such as clay minerals [2–5], biomaterials [6–9] and industrial solid wastes [10–13].

Sepiolite is a clay mineral, a complex magnesium silicate, a typical formula for which is $Mg_4Si_6O_{15}(OH)_2 \cdot 6H_2O$. Adsorption studies using modified sepiolite are relatively scarce. Adsorption is due to the presence of active adsorption centres on the sepiolite surfaces [14]. Sepiolite, which has a high surface area, should provide an efficient surface for the metal oxides. At the same time, the metal oxides can improve the Cu(II) adsorption capacity of sepiolite. The resulting composite adsorbent could become a very efficient way to remove Cu (II) from aqueous solution. To our knowledge, however, so far there has been no report in the literature of the study of the interaction between Cu(II) and iron oxide-coated sepiolite (ICS).

The aim of this paper is to examine the effectiveness of iron oxide-coated sepiolite (ICS) in removing Cu(II) from aqueous solution and to determine the adsorption characteristics of Cu(II) onto the ICS sample. Although several investigators have suggested applications for iron oxides in water and wastewater treatment [15–18], sepiolite has never been used as a support for iron oxide for heavy metal removal from wastewater. Due to this reason, ICS was proposed and studied in this research. For this aim, RS and ICS were examined in batch experiments for the removal of Cu(II) from aqueous solution (i.e. simulated wastewaters) in order to examine whether this separation technique may improve sepiolite performance as a Cu(II) adsorbent. The influence of pH, ionic strength, inorganic ligands (Cl^-, SO_4^{2-} and HPO_4^{2-}) and temperature on the adsorption of Cu(II) by the RS and ICS samples was investigated to better understand the Cu(II) adsorption process. The materials were characterized by infrared spectroscopy (IR), X-ray diffraction (XRD), and X-ray fluorescence (XRF) techniques.

2. Materials and methods

2.1. Materials

All reagents used, such as NaCl, $NaNO_3$, HNO_3, NaOH, and $Fe(NO_3)_3 \cdot 9H_2O$ were all of analytical grade and all solutions were prepared with double distilled water. A solution of 1.0 mM Cu(II) was prepared from $Cu(NO_3)_2 \cdot 5H_2O$ by dissolution in deionisied water. The stock was diluted to prepare a working solution.

The preparations of the iron oxide caoted clay sample have already been discussed in previous work [19]. The system was prepared by mixing 20.0 g of RS, 100 mL of freshly prepared 1.0 M $Fe(NO_3)_3 \cdot 9H_2O$ solution, and 180 mL of 2.0 M NaOH solution in a 2-L polyethylene flask. The addition of NaOH solution was rapid and with stirring. The

* Corresponding author. Tel.: +90 228 2160101; fax: +90 228 2160287.
E-mail address: erdal.eren@bilecik.edu.tr (E. Eren).

0011-9164/$ – see front matter © 2010 Elsevier B.V. All rights reserved.
doi:10.1016/j.desal.2010.05.039

suspension was diluted to 2 L with twice distilled water and was held in a pyrex glass beaker flask at 80 °C for 48 h.

Infrared (IR) spectra of the sepiolite samples were recorded in the region (4000 to 400) cm^{-1} on a Mattson-1000 FTIR spectrometer at a 4 cm^{-1} resolution. The mineralogical compositions of the RS and ICS samples were determined from the X-ray diffraction (XRD) patterns of the products taken on a Rigaku 2000 automated diffractometer using Ni filtered CuK_α radiation. The chemical analyses of sepiolite samples were carried out using a Rigaku ZSX Primus model XRF instrument.

2.2. Adsorption dependence on Cu(II) concentration

The experiments of adsorption equilibrium were carried out in a similar fashion to that described before [20]. A solution of 3.0 mM Cu (II) was prepared from $Cu(NO_3)_2 \cdot 5H_2O$ by dissolving in deionisied water. The stock was diluted to prepare a working solution of Cu(II). The background electrolyte solutions were 0.01 M, 0.1 M, and 0.5 M $NaNO_3$. Solution pH was adjusted with 0.1 M HNO_3 or 0.1 M NaOH, such that the equilibrium solutions had pH values ranging from 2.0 to 5.3. Preliminary kinetic studies indicated that Cu(II) adsorption was characterized by a rapid initial adsorption (within 3 h) followed by a much slower, continious uptake. A 4-h contacting period was found to be sufficient to achieve equilibrium. The separation of the liquid from the solid phase was achieved by centrifugation at 4500 rpm for 20 min. Adsorbed Cu(II) was calculated from the difference between the Cu(II) initially added to the system and that remaining in the solution after equilibration by a Unicam 929 model flame atomic absorption spectrophotometer. The dilutions induced by the pH controls were considered while computing the amount of Cu(II) adsorbed. Cu(II) adsorption in the presence of Cl^-, SO_4^{2-}, and PO_4^{3-} was performed by equilibrating 0.05 g of sepiolite in 21 mL of 0.1 M KNO_3 background electrolyte, 6 mL of Cu(II) working solution, and 3 mL of a NaCl, Na_2SO_4, or a Na_2HPO_4 working solution (achieveing 0.01 M Cl^-, 0.01 M SO_4^{2-}, or 0.01 M PO_4^{3-}) in 50-mL polyethylene centrifuge tubes. These experiments were performed in duplicate.

2.3. Data processing

The adsorption percentage of Cu(II) was calculated by the difference of the initial and final concentration using the following equation:

$$R = (C_0 - C_e) \times 100 / C_0 \quad (1)$$

where C_0 is the initial concentration of Cu(II) solution (mg/L), C_e the equilibrium concentration of the Cu(II) solution (mg/L), R the retention of Cu(II) in % of the added amount.

The equilibrium data have been analyzed using the Langmuir and Freundlich isotherms and the characteristic parameters for each isotherm have been determined [21,22]. A clear review of the equations and their application is in the literature [19]. The data conform to the linear form of the Langmuir model [21] (Eq. (2)) expressed below:

$$C_e / q_e = C_e / q_m + 1 / K_L q_m \quad (2)$$

where C_e is the equilibrium concentration of Cu(II) (mg/L) and q_e is the amount of the Cu^{2+} adsorbed (mg) per unit of sepiolite (g). q_m and K_L are the Langmuir constants related to the adsorption capacity (mg/g) and the equilibrium constant (L/g), respectively.

The adsorption equilibrium data was also applied to the Freundlich model [22] (Eq. (3)) given below:

$$\log\ q_e = \log\ K_f + (1/n) \log\ C_e \quad (3)$$

where K_f and n are the Freundlich constants related to adsorption capacity and adsorption intensity, respectively. The Freundlich parameters (K_F and n) indicate whether the nature of adsorption is either favorable or unfavorable.

The thermodynamic parameters of the adsorption process can be determined from the experimental data as described before [20]. The amount of Cu(II) ions adsorbed at equilibrium at different temperatures is 298, 308, 318 and 328 K, which have been examined to obtain the thermodynamic parameters for the adsorption system.

$$\ln K_d = \Delta S / R - \Delta H / RT \quad (4)$$

$$\Delta G = \Delta H - T\Delta S \quad (5)$$

$$K_d = q_e / C_e \quad (6)$$

where K_d is the distribution coefficient for the adsorption, ΔS, ΔH and ΔG are the changes of entropy, enthalpy and Gibbs energy, T (K) is the temperature, R (J mol^{-1} K^{-1}) is the gas constant. The values of ΔH and ΔS were determined from the slopes and intercepts of plots of ln K_d vs. 1/T.

The pseudo-first-order model was presented by Lagergren [23]. The Lagergren's first-order reaction model is expressed as follows:

$$\log(q_e - q_t) = \log q_e - (k_1 / 2.303)t \quad (7)$$

where q_t is the amounts of Cu(II) (mg/g) adsorbed on the sepiolite at time t, and k_1 is the rate constant (1/min). The rate constant, k_1 was obtained from slope of the linear plots of $\log(q_e - q_t)$ against t.

The sorption data was also analyzed in terms of pseudo-second-order mechanism, as described by Ho and McKay [24]:

$$t / q_t = (1/h) + (1/q_e)t \quad (8)$$

and the initial rate of adsorption h is:

$$h = k_2 q_e^2 \quad (9)$$

where k_2 is the rate constant of pseudo-second-order adsorption (g/mg min), h is the initial rate of adsorption (mg/g min). If second-order kinetics is applicable, the plot of t/q_t against t of Eq. (8) should give a linear relationship from which the constants q_e, h and k_2 can be determined.

In adsorption systems where there is the possibility of intraparticle diffusion being the rate-limiting step, the intraparticle diffusion approach described by Weber and Morris [25] is used. This equation can be described as (Eq. (7))

$$q_t = k_i t^{1/2} + C \quad (10)$$

where k_i (mg/g $min^{1/2}$) is the rate constant for intraparticle diffusion, and C (mg/g) is the intercept.

3. Results and discussion

3.1. Material characterization

The chemical analysis shows an decrease in the content of Mg^{2+} in the iron oxide-coated sepiolite in comparison with the raw sepiolite (Table 1). Taking into account that the percentages for each element are relative, and therefore, they are not adequate for making comparisons among samples, the ratios of Si/Mg are used for the

Table 1
Chemical composition of the sepiolite samples.

Sample	MgO	Al_2O_3	SiO_2	Fe_2O_3	CaO	NiO	SO_3	K_2O	Na_2O	P_2O_5	LOI
RS	30.24	0.42	54.81	0.22	0.43	0.25	0.02	0.05	–	0.01	13.56
ICS	23.91	0.37	49.73	15.45	0.24	0.24	0.03	0.02	5.40	–	4.61

analysis. The Si can be taken as a reference element due to it is a structural element of the sepiolite. Coating of the RS with iron oxide resulted in an increase of SiO_2/MgO ratio from 1.81 to 2.08 wt.%. It is most likely that the extraction of Mg^{2+} cations from octahedral positions under the working conditions applied during the coating process. Coating of RS with iron oxide resulted in the increase of Fe_2O_3 content from 0.22 to 15.45 wt.%. The loss on ignition (LOI) comes from the total water of minerals, carbonates and organic matter. There was a significant difference in LOI values of the RS and ICS. It is most likely that different types of water molecules from layers were removed during the thermal activation procesess of iron saturated sepiolite sample.

The XRD patterns of RS and ICS samples were presented in Fig. 1. For the XRD pattern of RS, main reflection was observed in the region $2°<2\theta<8°$ (Fig. 1a). This corresponds to the 7.10 (2θ) value from which the interlamellar distance was found to be 12.44 Å. The XRD results show that iron oxide-coating process has caused structural changes in the sepiolite sample. The position of d_{110} peak of RS sample shifted from 7.10 to 7.14 Å (Fig. 1b) which was accompained by a intensity decrease from 129 to 65.5 (Table 2). The formation of a new structure was illustrated by the peak appearing at lower <4.40° (20.06 Å) in the XRD pattern of the RS. The XRD peak intensities for ICS is less than those for some of the peaks for RS. Iron oxide-coating process of the RS has reduced mainly the intensities of the 110, 131 and 082 reflections, and the 370, 441 and 321 reflections of RS disappeared after oxide-coating process. It is known that XRD intensity is closely related with the crystallinity and particle size of the sample. The decrease of peak intensity in XRD pattern of ICS points out that iron oxide could be dispersed in the internal structure of sepiolite. This may be the reason for the broader and less intense peaks of the ICS sample compared with that for RS. Thus, the broader and less intense peaks for the ICS sample show its smaller crystal size and poorer crystal structure. In addition to this, introduction of the iron into the channels of sepolite may also decrease the crystallinity of the sepiolite.

Table 2
d-spacing and intensity values of reflections for sepiolite samples.

Reflection	RS		ICS		Ref. [26,27]
	d, Å	*I*	*d*, Å	*I*	
d_{110}	12.44	129	12.37	65.5	12.07
d_{130}	7.51	2.4	7.43	2.4	7.48
d_{131}	4.36	16.9	4.31	4.1	4.30
d_{260}	3.74	6.7	3.74	4.1	3.74
d_{080}	3.32	6.0	3.35	7.3	3.37
d_{370}	2.89	7.4	–	–	2.92
d_{441}	2.59	16.2	–	–	2.61
d_{321}	2.25	5.9	–	–	2.26
d_{082}	2.10	19.6	2.05	1.6	2.07

The IR spectra of the RS and ICS samples are presented in Fig. 2. The bands in the IR spectrum of RS (Fig. 2a) may be summarised as follows: (i) the band of the triple bridge group Mg_3OH is at 3686 cm^{-1}; (ii) the absorption of the structurally bound water is seen at 3560 cm^{-1}; and (iii) the stretches at 3428 cm^{-1} and the OH-bending mode at 1660 cm^{-1} are associated with zeolitic water. The lattice vibrations are given as follows: (a) the Si–O combination bands at (1207, 1072 and 967) cm^{-1}; (b) the basal plane of the tetrahedral units exhibiting the Si–O–Si plane vibrations at (1014 and 474) cm^{-1}, and (c) Mg_3OH bending vibration at 647 cm^{-1} [28]. Noticeable changes were detected for bands which are related to the OH vibrations in the region between 3700 and 3000 cm^{-1}. As the RS altered to ICS, changes in the IR absorption bands of the sample were noted at 3687, 3561, and 3428 cm^{-1} (Fig. 2b). The broad band at 3561 cm^{-1}, due to the zeolitic water in the RS, disappeared upon modification. It is also known that intermolecular hydrogen bonding causes the appearance of bands at 3550–3200 cm^{-1}. The band at about 3450 cm^{-1} results from monomeric structures, whereas the absorption near 3200 cm^{-1} arises from "polymeric" structures [29–31]. For the ICS sample, the bands at 3687, 3561 and 3428 cm^{-1} were replaced by a broad band at 3436 cm^{-1}. The broad band at 3436 cm^{-1} for ICS sample indicates the monomeric hydrogen bond vibrations. The observed shift toward lower frequency points out the increase in hydrogen bonding for ICS. Doula [31] and Cornell [32] agree that the

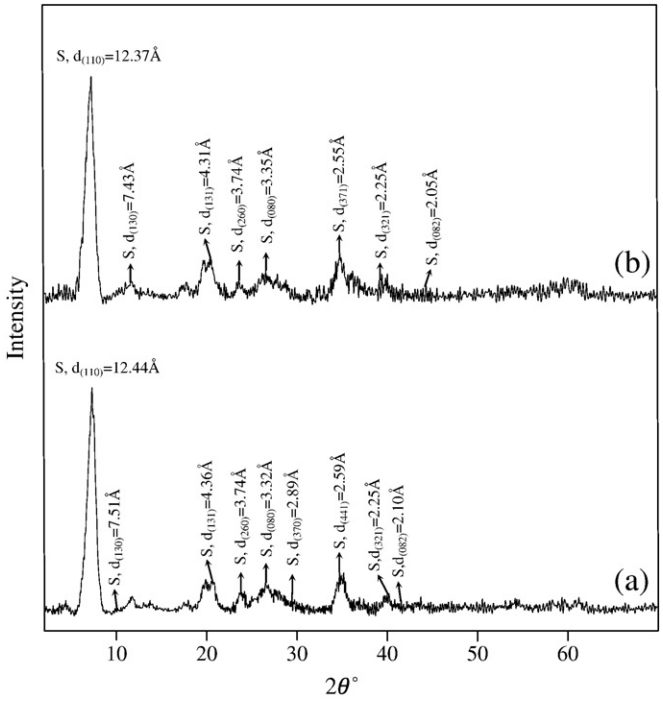

Fig. 1. The X-ray diffraction patterns of the RS (a) and ICS (b) samples (S: sepiolite).

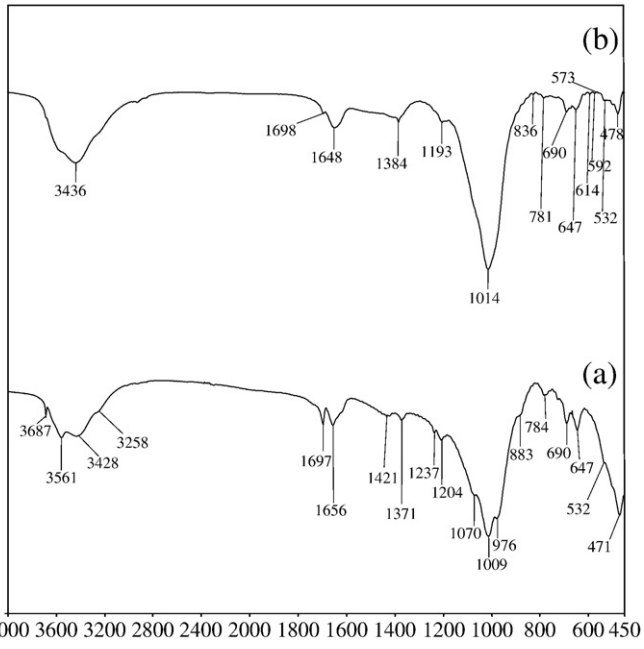

Fig. 2. IR spectra of the RS (a) and ICS (b) samples.

surface iron atoms, not structurally hydroxylated, complete their coordination shell of nearest neighbors through reaction with water in an aqueous medium as follows:

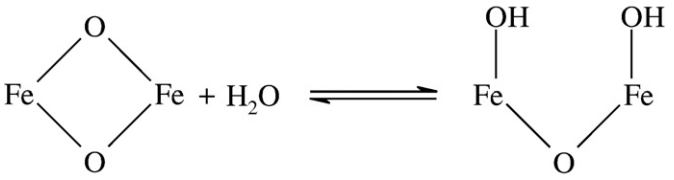

In the water-bending vibrational region, two partially resolved peaks at 1697 cm^{-1} and 1656 cm^{-1} which correspond to bending vibration of absorbed and zeolitic water for RS sample, respectively, were observed. The position of zeolitic water band shifted from 1656 to 1648 cm^{-1} after iron oxide coating process. The absorbance at 1698 cm^{-1} is weaker than corresponding absorbances for the RS, suggesting the decrease of the absorbed water content with the replacement of the introduced iron species. As shown in Fig. 2b, a new sharp band at 1384 cm^{-1} is observed for ICS sample. It may correspond to NO_3^-. Observed NO_3^- vibration band indicated that there are positively charged iron species outside the interlayer of sepiolite. For this reason, the NO_3^- anions act as counter ions to balance the positive charge of the iron species. The Si–O stretching band of RS at 1009 cm^{-1} became sharp and shifted to 1014 cm^{-1} after iron oxide coating process. The band centered at 1014 cm^{-1} for ICS can be attributed to the presence of Si–O–Fe bond. The absorption bands at 614, 592, and 573 cm^{-1} for ICS sample revealed the existence of a new iron oxide phase.

3.2. Adsorption isotherms and parameters

The effect of temperature on the adsorption equilibrium was investigated under isothermal conditions in the temperature range of 298–328 K (Figs. 3–6). As given in Table 3, the temperature of solution plays an important role in the whole adsorption process. The regression results demonstrated that the Langmuir isotherm fitted the experimental data better than the Freundlich. The Langmuir monolayer adsorption capacities varied from 14.96 to 31.84 mg/g (RS), 21.56 to 44.52 mg/g (ICS) in temperature range 298–328 K. The increase of adsorption capacities of RS and ICS for Cu(II) ions with increase in temperature indicates the endothermic nature of the adsorption processes. It is known that the adsorption process takes place by two consequent processes fast diffusion and slow complexation. The increase in temperature not only increases the rate of diffusion of the Cu(II) ions present in the bulk solution to the sepiolite surfaces but also increases the rate of complexation with the functional groups present on the sepiolite surfaces. The adsorption constant, K_L, also increased from 0.05 to 0.18 L/mg for RS and that for ICS increased from 0.08 to 0.71 L/mg with increasing temperature from 298 to 328 K. The higher K_L values for the ICS sample compared to that for RS indicate that the iron oxide-coating process influences the adsorption equilibrium. The high-energy sites with high equilibrium constant (K_L for ICS) had a significantly higher affinity than that for low-energy sites with low equilibrium constant (K_L for RS). The low-energy sites on which Cu(II) was loosely held had a low adsorption maximum (q_m = 14.96 mg/g for RS at 298 K). The high-energy sites on which dye were tightly held had a high adsorption maximum (q_m = 21.56 mg/g for ICS at 298 K). The maximum adsorption capacity of Cu(II) on iron oxide-coated sepiolite sample is approximately 1.44 times higher than that for the raw material.

The equilibrium data also fitted to Freundlich equation (Figs. 5 and 6), a fairly satisfactory empirical isotherm can be used for non-ideal adsorption. K_F relates the multilayer adsorption capacity and n intensity of adsorption, which varies with the heterogeneity of the adsorbent [33–36]. A relatively $n \ll 1$ indicates that adsorption intensity is favorable over the entire range of concentrations studied,

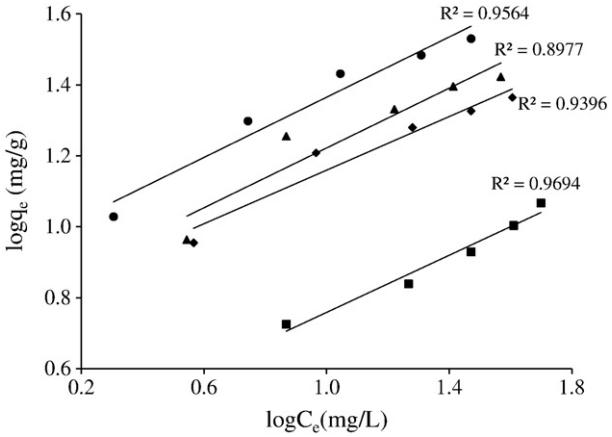

Fig. 4. Freundlich isotherm plot for the adsorption of Cu(II) onto RS sample at different temperatures. Squares, 298 K; diamonds, 318 K; triangles, 318 K; circles, 328 K, initial pH = 5.0, m = 1 g/L, ionic strength (IS) is 0.1 M $NaNO_3$ (controlled by $NaNO_3$).

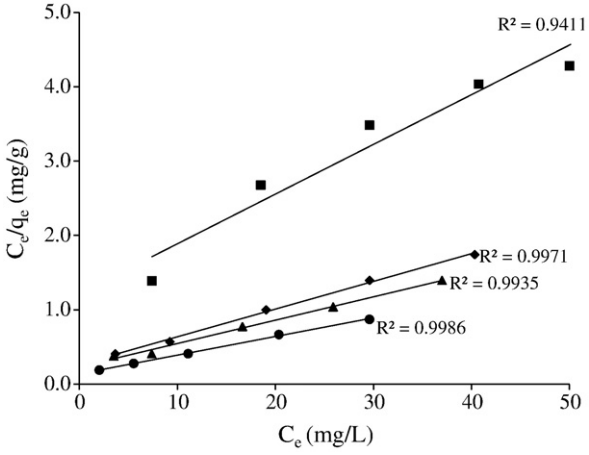

Fig. 3. Langmuir isotherm plot for the adsorption of Cu(II) onto RS sample at different temperatures. Squares, 298 K; diamonds, 318 K; triangles, 318 K; circles, 328 K, initial pH = 5.0, m = 1 g/L, ionic strength (IS) is 0.1 M $NaNO_3$ (controlled by $NaNO_3$).

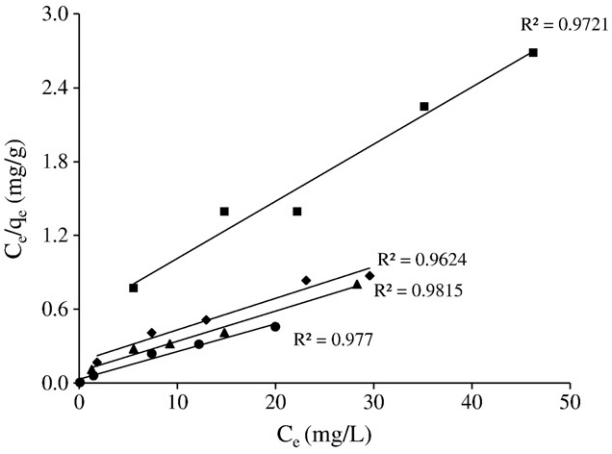

Fig. 5. Langmuir isotherm plot for the adsorption of Cu(II) onto RS sample at different temperatures. Squares, 298 K; diamonds, 318 K; triangles, 318 K; circles, 328 K, initial pH = 5.0, m = 1 g/L, ionic strength (IS) is 0.1 *M* $NaNO_3$ (controlled by $NaNO_3$).

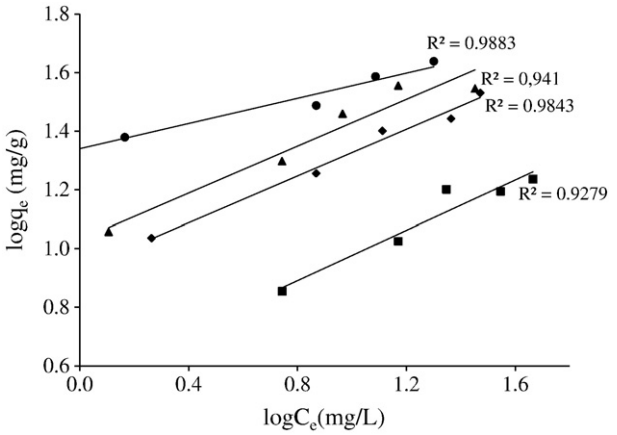

Fig. 6. Freundlich isotherm plot for the adsorption of Cu(II) onto RS sample at different temperatures. Squares, 298 K; diamonds, 318 K; triangles, 318 K; circles, 328 K, initial pH = 5.0, m = 1 g/L, ionic strength (IS) is 0.1 M $NaNO_3$ (controlled by $NaNO_3$).

while $n>1$ means that adsorption intensity is favorable at high concentrations but much less at lower concentrations [36,37]. The Freundlich adsorption capacity (K_F) for the RS sample was found to be lower than that for the ICS. In the adsorption systems, the n values are higher than 1 which point out that adsorption intensity is favorable at high concentrations.

There are few works related to Cu(II) adsorption on raw and modified sepiolite which have been reported [38–41]. Sancheza et al. [38] have reported that the maximum retention capacity for Orera sepiolite was obtained as 6.9 mg/g for Cu(II). Aminopropyltriethoxysilane modified sepiolite was reported to be 9.22 mg/g for the removal of Cu(II) from aqueous solution by Ozkan et al. [39]. Dogan et al. [40] have reported that q_m for adsorption of Cu(II) on [3-(2-aminoethylamino)propyl]trimethoxysilane modified sepiolite sample is 11.88 mg/g. Doğan et al. [41] have reported a Langmuir monolayer capacity, q_m, of 30.61 mg/g for Cu(II) adsorption onto sepiolite. From these observations, it also appears that the surface properties of RS could be improved upon modification of iron oxide.

3.3. Effect of ionic strength, pH and inorganic ligand

The adsorption of Cu(II) onto the sepiolite samples as a function of ionic strength and pH was shown in Fig. 7a and b. The two sepiolite samples showed an identical behavior of increased uptake of Cu(II) per unit mass with gradulally increasing pH, and the shape of curves dependent on the sepiolite surfaces. The experiments, however, could not be done at pH>6.0 due to insoluble copper hydroxide starts precipitating from the solution.

Table 3
Langmuir and Freundlich isotherm parameters for the adsorption of Cu(II) onto sepiolite samples.

Sample	T (K)	Langmuir constants			Freundlich constants		
		q_m (mg/g)	K_L (L/mg)	R^2	n	K_F ((mg/g)(L/mg)$^{1/n}$)	R^2
RS	298	14.96	0.05	0.941	2.49	2.27	0.969
	308	26.82	0.14	0.997	2.65	6.06	0.939
	318	31.84	0.14	0.93	2.37	6.32	0.897
	328	39.83	0.18	0.98	2.37	8.73	0.940
ICS	298	21.56	0.08	0.972	2.33	3.53	0.984
	308	38.99	0.15	0.962	2.51	8.47	0.984
	318	40.91	0.26	0.981	2.51	10.69	0.939
	328	44.52	0.71	0.976	4.65	21.88	0.988

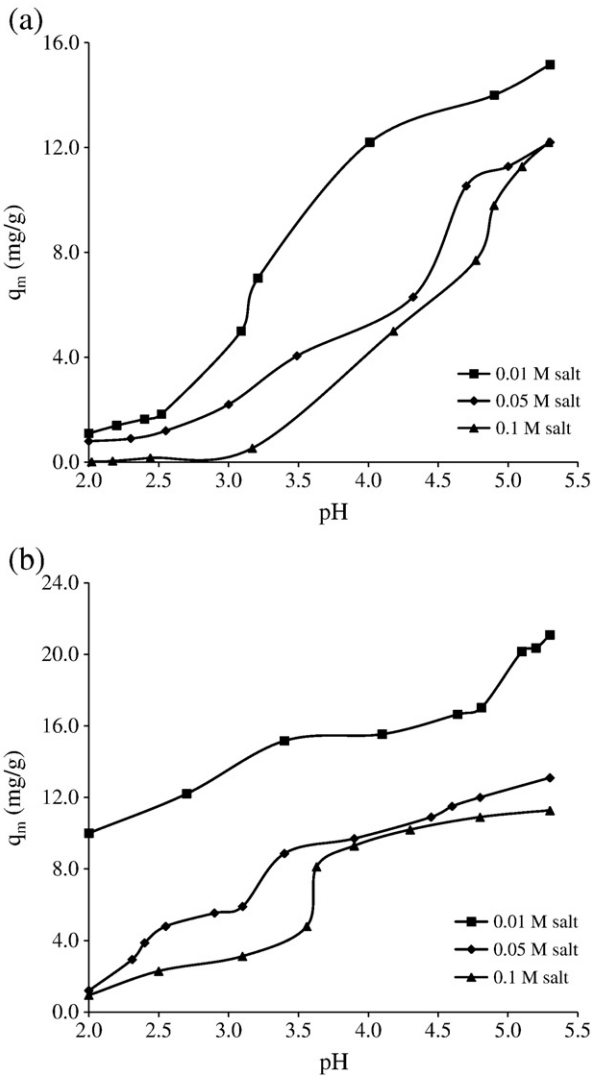

Fig. 7. a. Adsorption of Cu(II) (38.1 mg/L) by RS (1 g/L) as function of pH and ionic strength, squares, 0.1 M; diamonds 0.05 M; triangles,0.01 M. b. Adsorption of Cu(II) (38.1 mg/L) by ICS (1 g/L) as function of pH and ionic strength, squares, 0.1 M; diamonds 0.05 M; triangles,0.01 M.

The adsoption curve of RS have a different shape from that of ICS sample, and the adsorption capacity of this material is lower than ICS (Fig. 7a). The adsoption curve for this sample is characterized by one distinct adsorption edge. In the pH range 2.0 to 5.3, increasing ionic strength did not led to a significant change in the Cu(II) adsorption. The percent of Cu(II) adsorbed onto the RS sample in the presence of 0.01 M $NaNO_3$ at pH 6.5 is ≈39%, compared to 32% at the same pH but in the presence of 0.1 M $NaNO_3$.

As shown in Fig. 7b, Cu(II) adsorption by the ICS sample decreased when pH decreased. There is also a decrease in Cu(II) adsorption with increasing ionic strength. Increasing the ionic strength from 0.01 to 0.1 led to a significant decrease in the Cu(II) ions' adsorption for ICS sample. The percent of Cu(II) ions adsorbed in the presence of 0.01 M $NaNO_3$ at pH 5.3 is ≈55%, compared to 29% at the same pH but in the presence of 0.1 M $NaNO_3$ for the ICS sample. The adsoption curves for ICS are characterized by two distinct adsorption edges. For example, in the presence of 0.1 M $NaNO_3$, the first stage adsorption edge commenced at about 3% Cu(II) adsorption at pH ~2.0 and ended at pH ~3.5, at about which 5% of the total Cu(II) had been adsorbed. The second stage started at pH ~4.0 and continued up to pH 5.3 where

about 29% of the total Cu(II) was adsorbed. This may be due to the following two reasons: i—the effect of ionic strength on metal adsorption may be explained by the formation of outer-sphere complexes since Na^+ in the background electrolyte could compete with the copper ions adsorbed on the outer-sphere adsorption sites and reduced the adsorption, whereas Na^+ would not have competed for the inner-sphere sites. ii—The electrostatic attraction seems to be a significant mechanism, as indicated by the results where at high ionic strength, the increased amount of $NaNO_3$ can help render the surface of the ICS to be not easily accessible to Cu(II) ions. According to the electrical diffuse double layer theory, when solid adsorbent is in contact with sorbate species in solution, they are bound to be surrounded by an electrical diffused double layer, the thickness of which is significantly expanded by the presence of electrolyte. Such expansion may be inhibited between the approaching ICS particles and Cu(II) cations.

The adsorption of Cu(II) by the sepiolite samples was influenced by the presence of inorganic ligands (Fig. 8a and b). It points out that aqueous speciation by inorganic ligand influences Cu(II) adsorption.

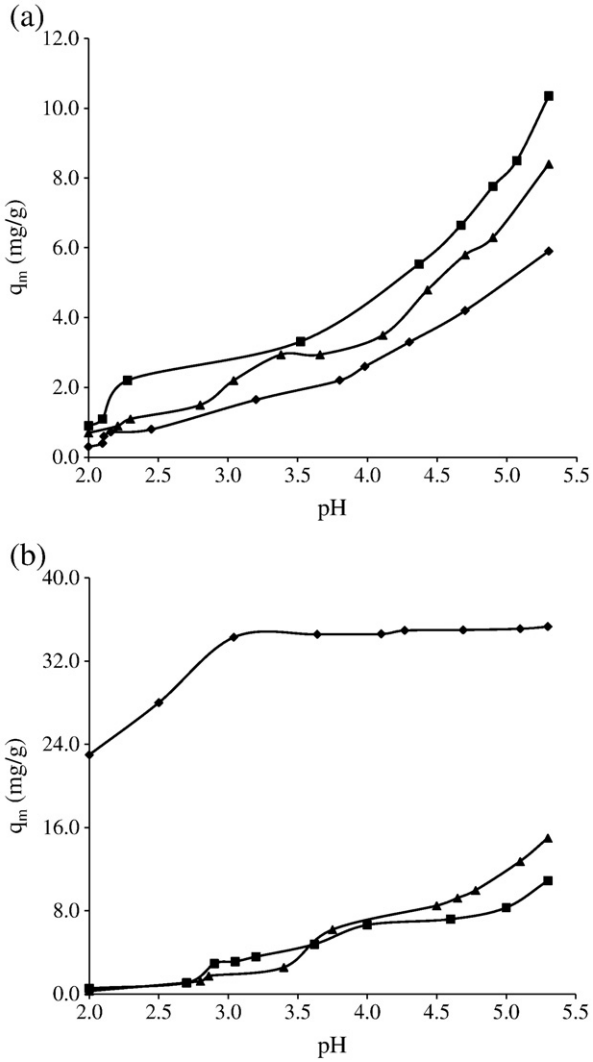

Fig. 8. a. Adsorption of Cu(II) (38.1 mg/L) by RS sample (1 g/L) as function of pH and in the presence of inorganic ligands. [IS is 0.1 M ($NaNO_3$)], squares, Cl^-; diamonds, SO_4^{2-}; triangles, HPO_4^{2-}. b. Adsorption of Cu(II) (38.1 mg/L) by ICS sample (1 g/L) as function of pH and in the presence of inorganic ligands. [IS is 0.1 M ($NaNO_3$)], squares, Cl^-; diamonds, SO_4^{2-}; triangles, HPO_4^{2-}.

The adsorbed Cu(II) in the presence of ligands may also be attributed to a high specifity of the surfaces for Cu(II).

As shown in Fig. 8a, the retention of Cu(II) ions by RS surface was decreased in the presence of 0.01 M inorganic ligands. The decreased amount of adsorbed Cu(II) ions can be explained in terms of solution chemistry. These ions effectively decrease the degree of hydrolysis of Cu(II) ions by blocking some of the coordination positions. Also, the reduction in Cu(II) ions' adsorption on the RS sample in the presence of Cl^-, SO_4^{2-} and HPO_4^{2-} might be due to ion competition with the various Cu(II) species for adsorption sites {e.g. [XOH^+–Cl^-, XOH^+–SO_4^{2-} and XOH^+–HPO_4^{2-}]}.

The adsorption of Cu(II) ions by the ICS sample was influenced by the presence of SO_4^{2-} and HPO_4^{2-} (Fig. 8b). The percent of Cu(II) ions adsorbed in the 0.01 M SO_4^{2-} and HPO_4^{2-} systems at pH 5.3 are 92 and 33%, respectively, compared to 29% at the same pH but in the absence of these ligands. This result suggests that the observed Cu(II) ions' adsorption behavior in the ICS suspensions is influenced by both aqueous speciation and surface ligand complexation of Cu(II) ions. The specifically adsorbed ligand enhances Cu(II) ions' retention by the surface complexation of Cu(II) ions. The increased amount of adsorbed Cu(II) on ICS can be explained in terms of solution chemistry, because Cu–L (L: SO_4^{2-} or HPO_4^{2-}), and CuOH–L complexes are the dominant Cu(II) species in the presence of 0.01 M SO_4^{2-} or HPO_4^{2-}. Thus, the specifically adsorbed ligand enhances Cu(II) retention by the surface complexation of Cu(II). Fig. 6 also showed that the retention of Cu(II) ions by ICS surface was not changed in the presence of 0.01 M Cl^- ligand. In the ICS suspensions, the percent of Cu(II) ions adsorbed in the 0.01 M Cl^- system at pH 5.3 is 28%, at the same pH but in the absence of the Cl^- ligand this value is 29%.

3.4. Thermodynamic studies

ΔG, ΔH, and ΔS were evaluated at 298 K for RS and ICS as −11.14 kJ/mol, 39.03 kJ/mol and 178 J/mol K; −16.09 kJ/mol, 32.99 kJ/mol and 165 J/mol K, respectively (Table 4). The negative values for the Gibbs energy change, ΔG, show that the adsorption process for the two sepiolite samples is spontaneous and the degree of spontaneity of the reaction increases with increasing tempreature. The values of ΔG are more negative for the ICS suggesting that the adsorption process for this material is more spontaneous. This observation suggests that the internal domains of this samples are more suitable environments for Cu(II) cations than the RS sample. Weng et al. [42] noted that ΔG° values up to 20 kJ/mol are consistent with electrostatic interaction between adsorption sites and the metal ion while ΔG° values more negative than 40 kJ/mol involve charge sharing or transfer from the adsorbent surface to the metal ion to form a coordinate bond. The values of ΔG obtained in this work, indicate that electrostatic interaction may play a significant role in the adsorption process. It may be suggested that a surface complexation reaction is the major mechanism responsible for the Cu(II) adsorption process. The heats of adsorption were calculated as positive for sepiolite samples. These positive values of ΔH suggest that a large amount of heat is consumed to transfer the Cu(II) ions from aqueous solution into the solid phase. As was suggested by Nunes and Airoldi

Table 4
Thermodynamic parameters for the adsorption of Cu(II) (51 mg/L) onto sepiolite samples.

Sample	ΔH (kJ/mol)	ΔS (J/molK)	ΔG (kJ/mol)				R^2
			298	308	318	328	
RS	39.03	178	−14.14	−15.92	−17.70	−19.49	0.855
ICS	32.99	165	−16.09	−17.74	−19.39	−21.03	0.963

Table 5
Kinetic parameters for the adsorption of Cu(II) onto a sepiolite samples. Contact time 300 min, $C_0 = 38.1$ mg/L, initial pH 5, and m = 1 g/L, ionic strength was controlled by 0.1 *M* $NaNO_3$.

Sample	Pseudo-first-order model	Pseudo-second-order model			Intra-particle diffusion model		
	R_1^2	R_2^2	$q_{e,cal}$ (mg/g)	$k_2 \times 10^3$ (g/mg min)	k_i (mg/g $min^{1/2}$)	C (mg/g)	R_i^2
RS	0.912	0.999	34.3	19	0.15	31.6	0.878
ICS	0.849	0.999	35.4	24	0.16	33.1	0.857

[43], the transition metal ions must give up a larger share of their hydration water before they could enter the smaller cavities. Such a release of water from the divalent cations would result in positive values of ΔS. This mechanism of the adsorption of Cu(II) ions is also supported by the positive values of ΔS, which show that Cu(II) ions are less hydrated in the sepiolite layers than in the aqueous solution. Also, the positive value of ΔS indicates the increased disorder in the system with changes in the hydration of the adsorbing Cu(II) cations.

The experimental adsorption thermodynamic data of the present investigation are comparable with reported values. Weng et al. [42] have reported that ΔG°, ΔH° and ΔS° for adsorption of Cu(II) on spent activated clay have values of −26.85 kJ/mol, 14.51 kJ/mol, and 138.78 J/molK, respectively. Bhattacharyya and Gupta [44] calculated that ΔH° of Cu(II) adsorption on TBA-montmorillonite, ZrO-kaolinite and montmorillonite was 29.2, 50.5 and 50.7 kJ/mol, respectively. Lin and Juang [45] have found that ΔG, ΔH and ΔS for Cu(II) adsorption on surfactant modified montmorillonite are −9.66 kJ/mol, 7.05 kJ/mol, and 9.09 J/K mol, respectively. Yavuz et al. [46] have reported that ΔG°, ΔH° and ΔS° for adsorption of Cu(II) on kaolinite are 4.61 kJ/mol, 39.52 kJ/mol, and 0.117 J/K mol, respectively.

3.5. Adsorption kinetics

By testing the three plots of $\log(q_e - q_t)$ versus t, (t/q_t) versus t, and q_t versus $t^{1/2}$, the rate constants k_1, k_2, and k_i and correlation coefficients can be calculated and the results are shown in Table 5. As seen from Table 5, compared to the pseudo-first-order and intraparticle diffusion kinetic models, a good correlation coefficient (R^2) was obtained for the pseudo-second-order kinetic model, which indicates that Cu(II) adsorption onto sepiolite samples follows the pseudo-second-order rate expression. The fact that the second-order kinetics is the best fit model for the adsorption of Cu(II) onto sepiolites indicates that the behavior over a whole range of adsorption is in agreement with chemical adsorption being the rate-controlling step [24]. In addition, it is necessary to note that the intercept (C) as proposed by Eq. (10) was not zero but a large value (31.6 and 33.1 mg/g for RS and ICS, respectively), indicating that intraparticle diffusion may not be the controlling factor in determining the kinetics of the process.

4. Conclusions

In the present work, a cheap, readily available and effective adsorbent material has identified sepiolite as a potentially attractive adsorbent for the treatment of Cu(II) contaminated aqueous solutions after modification with iron oxide. The adsorption of Cu(II) by sepiolite samples was influenced by pH, ionic strength, and the presence of inorganic ligands. The adsorption isotherm studies indicate that the adsorption of Cu(II) follows both the Langmuir and Freundlich isotherms. From the values of the Langmuir monolayer capacity, q_m, it is concluded that the treatment with iron oxide does increase the number of adsorption sites to a large extent. Since there is a huge deposit of sepiolite in Turkey, there is a great potential for its utilization in wastewater treatment.

References

[1] S. Veli, B. Alyüz, J. Hazard. Mater. 149 (2007) 226–233.
[2] G.A. Castro, M.G. Echegarrua, M.A. Perez, R. Moreno-Tost, E. Rodrıguez-Castellon, A. Jimenez-Lopez, Micropor. Mesopor. Mat. 108 (2008) 325–332.
[3] D. Karamanis, P.A. Assimakopoulos, Water Res. 41 (2007) 1897–1906.
[4] O. Khazali, R. Abu-El-Halawa, K. Al-Sou'od, J. Hazard. Mater. B139 (2007) 67–71.
[5] C.L. Peacock, D.M. Sherman, Geochim. Cosmochim. Ac. 69 (2005) 3733–3745.
[6] M. Kazemipour, M. Ansari, S. Tajrobehkar, M. Majdzadeh, H.R. Kermani, J. Hazard. Mater. 150 (2008) 322–327.
[7] S. Larous, A.-H. Meniai, M.B. Lehocine, Desalination 185 (2005) 483–490.
[8] A. Hammaini, F. Gonzalez, A. Ballester, M.L. Blazquez, J.A. Munoz, Miner. Eng. 16 (2003) 723–729.
[9] S. Lu, S.W. Gibb, Bioresour. Technol. 99 (2008) 1509–1517.
[10] B.M.W.P.K. Amarasinghe, R.A. Williams, Chem. Eng. J. 132 (2007) 299–309.
[11] Y.-H. Huang, C.-L. Hsueh, H.-P. Cheng, Su. L-C, C.-Y. Chen, J. Hazard. Mater. 144 (2007) 406–411.
[12] A. Papandreou, C.J. Stournaras, D. Panias, J. Hazard. Mater. 148 (2007) 538–547.
[13] I.J. Alinnor, Fuel 86 (2007) 853–857.
[14] A. Yebra-Rodriguez, J.D. Martin-Ramos, F. Del Rey, C. Viseras, A. Lopez-Galindo, Clay Miner. 38 (2003) 353–360.
[15] C. Boukhalfa, Desalination 250 (2010) 428–432.
[16] V. Zaspalis, A. Pagana, S. Sklari, Desalination 217 (2007) 167–180.
[17] M. Ozmen, K. Can, G. Arslan, A. Tor, Y. Cengeloglu, M. Ersoz, Desalination 254 (2010) 162–169.
[18] A. Dimirkou, M.K. Doula, Desalination 224 (2008) 280–292.
[19] E. Eren, J. Hazard. Mater. 165 (2009) 63–70.
[20] E. Eren, J. Hazard. Mater. 159 (2008) 235–244.
[21] I. Langmuir, J. Am. Soc. 40 (1918) 1361–1403.
[22] H. Freundlich, Zeitschrift für Physikalische Chemie (Leipzig) 57 (1906) 385–470.
[23] S. Lagergren, Kungliga Svenska Vetenskapsakademiens Handlingar 24 (1898) 1–39.
[24] Y.S. Ho, G. McKay, J. Environ Sci Health A 34 (1999) 1179–1204.
[25] W.J. Weber, J.C. Morris, J. Sanit. Eng. Div. Am. Soc. Civ. Eng. 89 (1963) 31–60.
[26] T. Irkec, T. Unlu, Min. Res. Expl. Bull. 115 (1993) 49–68.
[27] J.L. Post, S. Crawford, Appl. Clay Sci. 36 (2007) 232–244.
[28] A. Tabak, E. Eren, B. Afsin, B. Caglar, J. Hazard. Mater. 161 (2008) 1087–1094.
[29] R. Silverstein, G.C. Bassler, T.C. Morill, Spectromatic İdentification of Organic Compounds, Wiley & Sons, New York, 1981.
[30] M. Doula, A. Ioannou, A. Dimirkou, J. Colloid Interface Sci. 245 (2002) 237–250.
[31] M.K. Doula, Chemosphere 67 (2007) 731–740.
[32] mbH: D-69451. R.M. Cornell, U. Schwertmann, The İron Oxides, Structure, Properties, Reactions, Occurrence and Uses, VCH Verlagsgesellschaft, Weinheim, Germany, 1996.
[33] Y. Onal, C. Akmil-Basar, C. Sarıcı-Özdemir, J. Hazard. Mater. 148 (2007) 727–734.
[34] P. Balaz, A. Alacova, J. Briancin, Chem. Eng. J. 114 (2005) 115–121.
[35] Y.E. Mouzdahir, A. Elmchaouri, R. Mahboub, A. ElAnssari, A. Gil, S.A. Korili, M.A. Vicente, Appl. Clay Sci. 35 (2007) 47–58.
[36] Y.S. Al-Degs, M.I. El-Barghouthi, A.A. Issa, M.A. Khraisheh, G.M. Walker, Water Res. 40 (2006) 2645–2658.
[37] B.H. Hameed, A.L. Ahmad, K.N.A. Latif, Dyes Pigments 75 (2007) 143–149.
[38] A. García-Sánchez, A. Alastuey, X. Querol, Sci. Total Environ. 242 (1999) 179–188.
[39] O. Demirbaş, M. Alkan, M. Doğan, Y. Turhan, H. Namli, P. Turan, J. Hazard. Mater. 149 (2007) 650–656.
[40] M. Doğan, Y. Turhan, M. Alkan, H. Namli, Pınar Turan, Ö. Demirbaş, Desalination 230 (2008) 248–268.
[41] M. Doğan, A. Türkyilmaz, M. Alkan, Ö. Demirbaş, Desalination 238 (2009) 257–270.
[42] C.-H. Weng, C.-Z. Tsai, S.-H. Chu, Y.C. Sharma, Sep. Purif. Technol. 54 (2007) 187–197.
[43] L.M. Nunes, C. Airoldi, Thermochim. Acta 328 (1999) 297–305.
[44] K.G. Bhattacharyya, S.S. Gupta, Sep. Purif. Technol. 50 (2006) 388–397.
[45] S.-H. Lin, R.-S. Juang, J. Hazard. Mater. 92 (2002) 315–326.
[46] O. Yavuz, Y. Altunkayank, F. Guzel, Water Res. 37 (2003) 948–952.